

Journal of Biomedical Optics

SPIDigitalLibrary.org/jbo

Detection of anthrax *lef* with DNA-based photonic crystal sensors

Bailin Zhang
Shatha Dallo
Ralph Peterson
Syed Hussain
Tao Weitao
Jing Yong Ye

Detection of anthrax *lef* with DNA-based photonic crystal sensors

Bailin Zhang,^a Shatha Dallo,^b Ralph Peterson,^a Syed Hussain,^a Tao Weitao,^b and Jing Yong Ye^a

^aUniversity of Texas at San Antonio, Department of Biomedical Engineering, San Antonio, Texas 78249

^bUniversity of Texas at San Antonio, Department of Biology, San Antonio, Texas 78249

Abstract. *Bacillus anthracis* has posed a threat of becoming biological weapons of mass destruction due to its virulence factors encoded by the plasmid-borne genes, such as *lef* for lethal factor. We report the development of a fast and sensitive anthrax DNA biosensor based on a photonic crystal structure used in a total-internal-reflection configuration. For the detection of the *lef* gene, a single-stranded DNA *lef* probe was biotinylated and immobilized onto the sensor via biotin-streptavidin interactions. A positive control, *lef-com*, was the complementary strand of the probe, while a negative control was an unrelated single-stranded DNA fragment from the 16S rRNA gene of *Acinetobacter baumannii*. After addition of the biotinylated *lef* probe onto the sensor, significant changes in the resonance wavelength of the sensor were observed, resulting from binding of the probe to streptavidin on the sensor. The addition of *lef-com* led to another significant increase as a result of hybridization between the two DNA strands. The detection sensitivity for the target DNA reached as low as 0.1 nM. In contrast, adding the unrelated DNAs did not cause an obvious shift in the resonant wavelength. These results demonstrate that detection of the anthrax *lef* by the photonic crystal structure in a total-internal-reflection sensor is highly specific and sensitive. © 2011 Society of Photo-Optical Instrumentation Engineers (SPIE). [DOI: 10.1117/1.3662460]

Keywords: biosensor; label-free detection; *Bacillus anthracis*; DNA hybridization.

Paper 11338R received Jun. 30, 2011; revised manuscript received Oct. 27, 2011; accepted for publication Oct. 31, 2011; published online Dec. 8, 2011.

1 Introduction

Bacillus anthracis (*B. anthracis*), a pathogen of a zoonotic infectious disease—anthrax, has posed a threat of becoming biological weapons of mass destruction (BWMD).¹ Such terrorization originates from the bacterial virulence factors. These factors include toxins and antiphagocytic capsular polypeptides.^{2,3} They are encoded by genes harbored in two virulence plasmids, pXO1 and pXO2.⁴ pXO1 carries the genes for three toxin proteins: *cya* for edema factor, *lef* for lethal factor, and *pagA* for protective antigen. These proteins, acting in binary combinations, cause edema and cell death in the host, but nontoxic alone.^{5,6} pXO2 harbors three genes essential for capsule synthesis.⁷ The capsule prevents phagocytosis of the vegetative bacterial cells and inhibits the host defense mechanisms.⁸ The vegetative bacilli armed with these virulent factors are culprits of the bacteremia and the lethal toxemia as well as the host response, responsible for the overt symptoms of the host; if untreated, the infected individuals die in a few days. These attributes rank *B. anthracis* high on the list of BWMD and demand rapid detection for early treatment to minimize casualties.

With the advent of bioterrorism, a variety of nucleic acid-based biosensors have been developed. This approach generally constitutes immobilization of DNA probes onto a transducer surface of the biosensor, capturing of DNA analytes through complementary base-pairing, and monitoring of the reaction signals. The fluorescently labeled DNA probes have long been used to generate the signals. The drawbacks of the fluorescence-based biosensing include high cost, background noise, and prolonged

operation time required for labeling. The effort to overcome the limits has stimulated the development of label-free biosensing technologies.^{9–20} Surface plasma resonance (SPR) techniques have been developed for anthrax detection with antibodies,²¹ but DNA-based SPR detection of anthrax has not been reported.

This work aims to develop a DNA-based biosensor for fast detection of anthrax DNA that is label-free, sensitive, specific, and easy to operate. It is based on a prototype of a photonic crystal structure in a total-internal-reflection (PC-TIR) we developed recently.^{22–24} The PC-TIR configuration creates a unique open microcavity allowing biomolecules to easily access the sensing surface. In this study, the *lef*-derived single-stranded (ss) DNA was immobilized on the sensor surface to recognize its complementary strand versus the unrelated DNA.

2 Experimental Procedures

2.1 Design and Fabrication of PC-TIR Sensors

We used the following optical sensor fabricated for detection of the *lef* DNA. Specifically, we conceptually split a Fabry–Pérot etalon with a cavity layer sandwiched between two PC structures from the middle and use only half of the structure in a TIR geometry [Fig. 1(a)]. Owing to the TIR, there is a mirror image of the PC structure [Fig. 1(b)]. Thus, even with only half a conventional etalon structure, a cavity is still formed between the PC structure and its imaginary part in the TIR configuration. It is important to note that this is an open cavity [Fig. 1(c)] in contrast to the closed cavity in a conventional etalon. The existence of resonant modes similar to that of a Fabry–Pérot etalon cavity

Address all correspondence to: Jing Yong Ye, University of Texas at San Antonio, Biomedical Engineering, One UTSA Circle, San Antonio, Texas 78249; Tel: 210-458-5056; E-mail: jingyong.ye@utsa.edu.

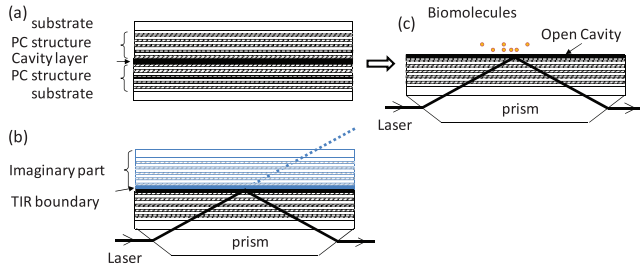


Fig. 1 Working principle of a PC-TIR sensor. (a) A cavity layer sandwiched by two pieces of PC structures. We conceptually split this structure from the middle layer into two pieces. (b) One piece of the PC structure is used in a TIR configuration. Owing to the TIR, an imaginary PC structure exists and a microcavity is still formed as if there were two pieces of the PC structures. (c) This PC-TIR sensor offers a unique sensing interface open for biomolecular assays.

has been verified in our previous experiments utilizing the open cavity for real-time bioassays.^{22–24}

We designed and fabricated a PC-TIR sensor based on the following theoretical calculations. The sensor is composed of a transparent substrate, a periodic structure of two alternating layers of different dielectric materials (silica and titania), and a polymer thin film as the cavity layer. Assume the incident angle at the substrate layer is θ_i , and the refraction angles in the substrate (S), silica (A), titania (B), and cavity layer (X) are θ_s , θ_A , θ_B , and θ_X , respectively. Let n_s , n_A , n_B , and n_X be the refractive index of the substrate, the silica, the titania, and the cavity layer, respectively. In order to form a photonic bandgap, the thickness of the dielectric multilayer has to satisfy,

$$d_A = \frac{\lambda_d}{4(n_A^2 - n_S^2 \sin^2 \theta_S)^{1/2}}, \quad d_B = \frac{\lambda_d}{4(n_B^2 - n_S^2 \sin^2 \theta_S)^{1/2}}, \quad (1)$$

where d_A and d_B are the thickness for silica and titania, respectively. λ_d is the selected resonant wavelength, which was 632.8 nm in this experiment. An incident angle θ_s was chosen to be 64 deg. At this incident angle, titania and silica layers therefore have a designed thickness of 89.8 and 307.2 nm, respectively. They were used to form five alternating layers of the PC structure and fabricated with electron-beam physical vapor deposition on a BK7 glass substrate.

For obtaining a resonance condition in the cavity, the thickness of the cavity layer d_x should satisfy the following relation:

$$2 \cdot \frac{2\pi}{\lambda_d} n_x d_x \cos \theta_x + \alpha = (2m + 1)\pi \quad (m = 0, 1, 2, \dots), \quad (2)$$

where α represents the Goos–Hänchen phase shift. The factor of 2 in the first term on the left-hand side is due to the fact that the light double passes this layer owing to the TIR. The integer m means multiple resonant conditions can be satisfied. For s -polarization of incident light, substituting the Goos–Hänchen phase shift expression into Eq. (2), one obtains the thickness of the cavity layer:

$$d_x = \frac{\lambda_d}{4\pi(n_x^2 - n_S^2 \sin^2 \theta_S)^{1/2}} \left\{ 2m\pi + \pi - 2 \tan^{-1} \times \left[\frac{(n_S^2 \sin^2 \theta_S - n_H^2)}{n_x^2 - n_S^2 \sin^2 \theta_S} \right]^{1/2} \right\}, \quad (3)$$

where n_H is the refractive index of the medium above the cavity layer. The cavity layer of the sensor was formed with a thin film (~ 330 nm) of poly(methyl methacrylate) (PMMA) (A6, MicroChem), which was spin-coated on the PC structure at 500 revolutions per minute (rpm) for 10 s, followed by 4200 rpm for 45 s. This sensor structure was baked at 60°C for 30 min.

2.2 Instrumentation of the PC-TIR Technology

Our instrumentation basically comprises the sensor chip, sample wells, a broadband light source, and two compact spectrometers. In particular, two sample wells were fabricated with polydimethylsiloxane (PDMS) and placed in contact with the top surface of the sensor chip. Each well has a diameter of 6 mm and a height of 8 mm. A broadband white light source was coupled to a single-mode optical fiber to obtain a high-quality spatial mode. The output beam from the fiber was collimated and passed through a linear polarizer to select s -polarization. The beam was split into two with a 50/50 beamsplitter and coupled to the PC-TIR sensor with a prism. The incident angle of the beams at the sensor substrate was adjusted to 64 deg. The two beams were aligned to the bottom of the two wells, respectively. The spectra of the beams reflected from the sensor were measured with two spectrometers to monitor the resonant wavelengths in the two channels, respectively. One of the channels was used as a signal channel, while the other as a reference channel to compensate any changes in the resonant wavelength due to mechanical drift or temperature fluctuations.

2.3 Selecting Oligonucleotides

Three 80-mer oligonucleotides of ssDNA were utilized in this study. The first was termed *lef*-probe selected from *lef*. The selection criteria were to choose low guanine and cytosine (GC) contents and minimal numbers of inverted repeats, so that melting would be facilitated and self-folding would be minimized during hybridization. The GC contents were 28%, and the basic melting temperature was 67.8°C. This probe was biotinylated at 5'-end. The sequences: 5'- AAA GTA GTG CCA AAG AGT AAA ATA GAT ACA AAA ATT CAA GAA GCA CAG TTA AAT ATA AAT CAG GAA TGG AAT AAA GCA TT-3'. The second was *lef*-com, which is complementary to *lef*-probe with the sequences: -3'- TTT CAT CAC GGT TTC TCA TTT TAT CTA TGT TTT TAA GTT CTT CGT GTC AAT TTA TAT TTA GTC CTT ACC TTA TTT CGT AA-5'. The third was the rDNA control selected from the gene encoding 16S rRNA of *Acinetobacter baumannii*. In addition to the above-mentioned selection criteria, the control DNA was selected by the lowest complementarity to *lef*-probe (8% identified by reverse comparison and 14% by forward comparison). The GC contents were 55%, and the basic melting temperature was 79°C. The sequences: 5'- TAACGCGATA AGTA-GACCGC CTGGGGAGTA CGGTCGCAAG ACTAAAACCT AAATGAATTG ACGGGGGCCC GCACAAGCGG -3'.

2.4 Functionalization of the PC-TIR Sensor

The sensor chip was functionalized through the following steps for detection of the *lef* gene (Fig. 2): 1. Aldehyde groups were introduced onto the PMMA surface of the sensor to enhance immobilization of streptavidin on the sensor surface.^{25–27} Briefly,

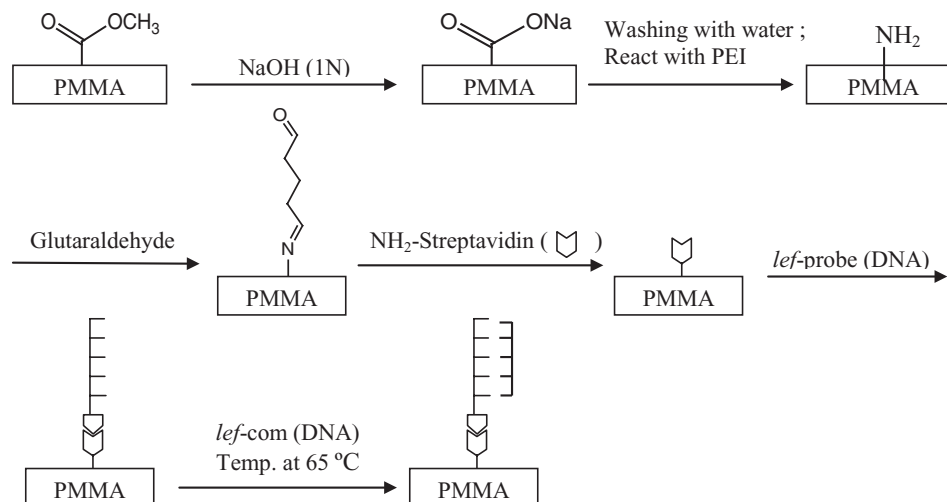


Fig. 2 Schematic illustration of the stepwise process involved in the surface modification and immobilization strategies for functionalization of the PC-TIR sensor surface.

the PMMA surface was partly hydrolyzed with NaOH solution at 1N for 30 min at 55°C, and then the surface was fully rinsed with deionized (DI) water until the pH value reached 7. The substrate was dried and immersed in poly(ethyleneimine) (PEI) (MW = 75,000, Sigma-Aldrich) solution (2.5%, pH = 7) at room temperature for 1 h. After washing with DI water, the aminated substrate surface was further immersed in a 2% (w/v) glutaraldehyde solution for 30 min at 25°C. The surface was rinsed with copious DI water and then dried. 2. The PDMS wells were placed on top of the chip by gently pressing them together. Each well was filled with a 200- μ l volume of phosphate buffered saline (PBS, pH 7). The resonant wavelengths of the two wells were measured and set as the detection baseline. 3. The PBS in the sample well was then replaced with 200- μ l PBS solution containing streptavidin (40 μ g/ml, from Invitrogen). After immobilization of streptavidin on the sensor surface had been completed, the well was washed twice with PBS. The amount of streptavidin bound to the sensor surface in a 200- μ l volume of PBS at 25°C after washes was measured by the resonant wavelength shift of the sensor. Different from the case that such washes largely removed streptavidin from the unmodified sensor surface, the strong association of streptavidin with the chemically-modified sensor suggests covalent bonding of streptavidin to the surface through interaction of amino groups of streptavidin with the aldehyde groups on the sensor surface as reported.^{25–27} 4. Biotinylated single-stranded *lef*-probe DNA (100 nM in 200 μ l PBS) was used to replace the PBS in the well for immobilization of the *lef*-probe on the surface via strong binding between streptavidin and biotin. After washed with PBS twice, the well was filled with 200- μ l PBS. The amount of the biotinylated *lef*-probe bound to the surface was quantified by measuring the resonant wavelength shift. The sensor chip was thus functionalized with the *lef* DNA and ready for hybridization.

2.5 Detection of Hybridization

lef-com (100 nM in 200 μ l PBS) was incubated at 65°C in the heating block for 5 min to minimize DNA self-folding. It was

then injected into the *lef*-functionalized sensor well immediately. After the temperature cooled down to 25°C, the well was washed twice with PBS. The amount of *lef*-com bound to the sensor surface was quantified by measuring the resonant wavelength shift of the sensor. The rDNA control was tested the same way as *lef*-com. The hybridization for the *lef*-com concentrations at 0.1, 1, and 100 nM were measured.

Finally, multiple pairs of controls were included and tested on the sensors. The first pair was free streptavidin versus PBS on the unmodified sensor showing that without the covalent immobilization, binding of streptavidin to the sensor were mostly lost after washes. The second was immobilized streptavidin versus free DNA indicating that without biotinylation, the free DNA was washed off after rinsing steps. The third was biotinylated DNA versus PBS on the modified sensor demonstrating that without immobilized streptavidin, the DNA probe was largely lost after washing.

3 Results

We initially encountered technical challenges when immobilizing DNA probes onto the PMMA surface of the biosensor. Since the net charge of the PMMA surface is negative while the avidin is highly positively charged at pH 7.4, it is possible to directly immobilize avidin molecules on the PMMA surface via electrostatic absorption. We observed near-full coverage of avidin monolayer on the sensor surface. However, the signal for hybridization between biotinylated *lef*-probe and *lef*-com was unexpectedly low (see Sec. 4 for details). One likely cause was that the negatively-charged *lef*-probe tends to lie flat on the positively-charged avidin-coated surface as a result of electrostatic attraction. This effect may have hindered the *lef*-com and *lef*-probe hybridization. To solve this problem, we used streptavidin. In contrast to avidin, streptavidin is negatively charged at pH 7.4, thus preventing negatively charged DNA molecules from lying flat on the sensor surface. However, because PMMA has the same sign of charges as streptavidin, immobilization of streptavidin on the PMMA surface cannot be achieved via electrostatic adsorption. We therefore intended to immobilize

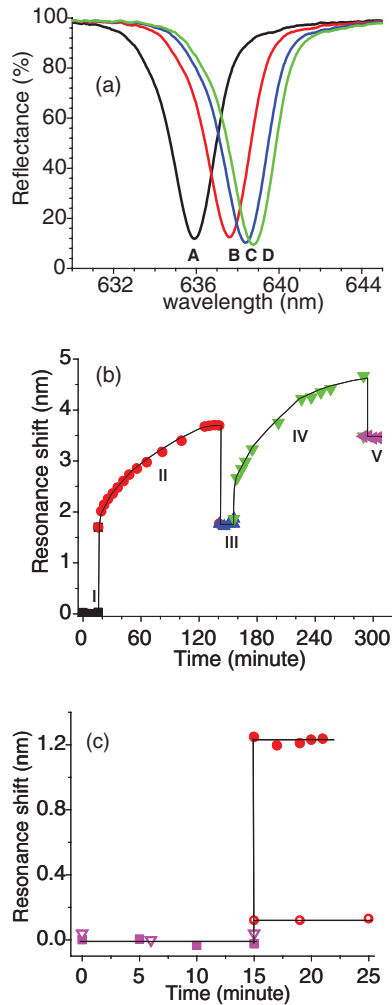


Fig. 3 Detection of *lef* by functionalized PC-TIR sensor. (a) Representative resonant reflectance spectra of the sensor. Curve A, PBS injected on the sensor surface. Curves B, C, and D, corresponding to the spectra taken at time 0, 20 min, and 40 min, respectively, after injection of streptavidin onto the sensor surface. There was an immediate change in the resonant wavelength at time 0 because of the difference of refractive indices between PBS and the streptavidin solution. (b) The binding curve of streptavidin on the PEI-treated sensor surface. At stage I: a PBS solution was injected into the sensor well; Stage II: the resonant wavelength change due to the binding of streptavidin molecules to the aldehyde groups on the PEI-modified sensor surface; Stage III: the remaining streptavidin molecules covalently bound to the sensor surface after rinsing; Stage IV: the binding kinetics of biotinylated *lef*-probe with streptavidin on the sensor surface; Stage V: the bound *lef*-probe remaining on the sensor surface after rinsing. (c) Hybridization of *lef*-probe with the complementary *lef*-com (solid circle) and an unrelated rDNA control (open circle).

streptavidin on the PEI-treated PMMA surface through covalent binding. Figure 3(a) shows several representative reflectance spectra of the sensor at different times during the immobilization of streptavidin. The spectra shift to longer wavelengths, indicating the increased amount of streptavidin immobilized on the sensor surface. Figure 3(b) plots the shift of resonant wavelength at different stages of the whole functionalization process of the sensor. The curve at stage I shows the detection baseline when PBS was injected on the sensor surface. The resonant wavelength started to shift when the buffer was replaced with

200- μ l streptavidin (200 μ g/ml in PBS) [Fig. 3(b) stage II]. The shift reached a plateau, indicative of the status of binding saturation. After washes, the curve at stage III shows the remaining streptavidin molecules bound to the surface.

The surface is then ready for attaching the biotinylated *lef*-probe. For that, a 200- μ l volume of the biotinylated *lef*-probe solution at a concentration of 100 nM in PBS was added to the sensor surface immobilized with streptavidin. The binding curve of the biotinylated *lef*-probe is shown at stage IV in Fig. 3(b). After the sensor surface had been washed with PBS to remove molecules with nonspecific binding, the resonant wavelength shift changed from 4.6 to 3.5 nm. The curve at stage V indicates the amount of the *lef*-probe molecules immobilized on the sensor surface. Hence, functionalization of the sensor chip was completed and the sensor was ready for anthrax DNA detection.

We tested the functionalized sensor for detection of DNA hybridization between the immobilized *lef*-probe and the targeted *lef*-com. The temperature of the 200- μ l *lef*-com solution (100 nM in PBS) was raised to 65°C before injection of the target ssDNA onto the *lef*-probe functionalized sensor surface in order to minimize formation of a secondary structure from ssDNA. After the temperatures had cooled down to allow *lef*-com to hybridize with the *lef*-probe on the sensor surface, the sensor was rinsed with PBS, and the reflectance spectra of the sensor were measured. Figure 3(c) demonstrates the resonant wavelength change of the sensor resulting from the binding of *lef*-com to *lef*-probe. Based on our transfer matrix simulation of multilayer interference,²³ the 1.2-nm shift in the resonant wavelength corresponds to an averaged binding thickness of 0.8 nm of *lef*-com on the sensor surface.

In addition to hybridization of the biotinylated *lef*-probe with its complementary DNA, the unrelated DNA was used to test specificity of the sensor for *lef* detection. When a 200- μ l volume of the rDNA control (100 nM in PBS) derived from *A. baumannii* was heated and injected as above, a shift of the resonant wavelength was only 0.2 nm, a reduction of 84% compared with *lef*-com [Fig. 3(c)]. The decrease most likely resulted from the reduced base-pairing between the *lef* probe and the rDNA control, given the fact of the low complementarities between the two ssDNAs. This result indicates that the functionalized PC-TIR sensor is highly specific in detection of anthrax DNA.

In order to determine the sensitivity of the sensor, different concentrations of *lef*-com were tested. The resonant wavelength shift of the sensor increased with increasing *lef*-com concentrations (Fig. 4). At 100 nM, the sensor response did not appear to increase linearly with the concentration of *lef*-com, suggesting binding saturation at this high concentration level. When the concentration of *lef*-com was as low as 0.1 nM, a clear response of the sensor was still observed.

4 Discussion

In this study, a sensitive photonic-crystal-based biosensor was fabricated to allow a unique open microcavity for rapid label-free biochemical assays. For detection of the *B. anthracis lef* gene, the sensor was functionalized with the synthetic ssDNA, *lef*-probe, from the plasmid-borne *lef* gene of *B. anthracis*. Significant changes in the resonant wavelength of the sensor were observed when the complementary strand, *lef*-com, was

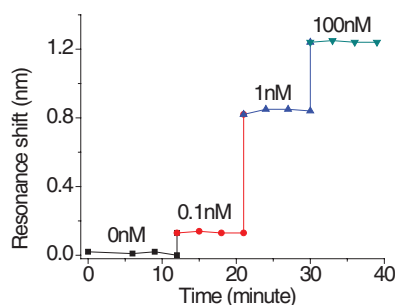


Fig. 4 Sensor responses to *lef-com* binding at concentrations of 0.1, 1.0, and 100 nM.

recognized by the sensor. The detection sensitivity was obtained to be better than 0.1 nM of *lef-com*. Specificity of the functionalized sensor has also been confirmed by using a negative control of an unrelated ssDNA fragment. These results demonstrate that detection of the anthrax *lef* gene with the PC-TIR sensor is highly specific and sensitive.

One of the technical challenges for the nuclei acid-based biosensing technology is immobilization of DNA probes onto a biosensor. We initially attempted to take advantage of the avidin-biotin approach to immobilization of DNA. The reason was that the negatively-charged PMMA surface and the positively-charged avidin at pH 7.4 allow direct immobilization of avidin onto the PMMA surface through electrostatic adsorption. After a 200- μ l volume of avidin (200 μ g/ml in PBS) was injected into the sample well on the PMMA surface, we observed that the resonant reflectance spectra of the sensor shifted as large as 5.5 nm, which indicates almost a full coverage of a monolayer of avidin on the sensor surface.²⁸ Biotinylated *lef*-probe molecules were then injected on the avidin immobilized sensor surface. A further shift of the resonant wavelength by 0.6 nm was observed due to the binding of *lef*-probe to the sensor surface. However, the resonant wavelength only shifted by 0.15 nm when a 200- μ l volume of *lef-com* (100 nM in PBS) was added onto the sensor surface. The data suggest that little hybridization of *lef-com* with *lef*-probe occurred on the sensor surface. One possible reason for the low hybridization rate may be attributed to the following facts. The immobilized avidin is positively charged at pH 7.4 while *lef*-probe is negatively charged so that electrostatic attraction may cause *lef*-probe to lie down on the avidin coated surface, hindering hybridization. Nevertheless, this problem was successfully solved in this study by immobilizing streptavidin via covalent binding.

The capability of directly detecting anthrax DNA is of high impact because it may allow further reconfiguration of the sensor for recognizing DNA not only in the vegetative cells but also in the endospores of *B. anthracis*. *B. anthracis* generates endospores, a dormant life form, while the vegetative form is aerobic, Gram-positive, and rod-shaped. The endospores are not only transmittable easily to humans but also resistant to harsh environments,²⁹ all of which have made the anthrax endospores a potential BWMD.³⁰ Once inhaled, the endospores are engulfed either by host defense cells where the spores germinate and assume vegetative forms. The vegetative bacterial cells are disseminated, causing septicemia and producing virulence factors. Thus, rapid detection of the endospores in the environments and the vegetative form of *B. anthracis* in human bodies is de-

manded so that early specific treatment can be administered to reduce fatalities. With the PC-TIR sensor functionalized for detecting anthrax DNA, we believe this work has demonstrated a significant progress in the label-free photonic-crystal biosensing technologies, a prerequisite for rapid detection of BWMD.

Acknowledgments

The fabrication of the PC-TIR sensor was partly supported by the SALSII grant funded through the American Recovery and Reinvestment Act. This work was also supported by San Antonio Area Foundation and UTSA Collaborative Research Seed Grant Program. Dr. Tao Weitao contributed to the original concept, experimental design, and manuscript writing.

References

- D. G. Bouzianias, "Current and future medical approaches to combat the anthrax threat," *J. Med. Chem.* **53**, 4305–4331 (2010).
- B. D. Green, L. Battisti, T. M. Koehler, C. B. Thorne, and B. E. Ivins, "Demonstration of a capsule plasmid in *Bacillus anthracis*," *Infect. Immun.* **49**, 291–297 (1985).
- P. Mikesell, B. E. Ivins, J. D. Ristroph, and T. M. Dreier, "Evidence for plasmid-mediated toxin production in *Bacillus anthracis*," *Infect. Immun.* **39**, 371–376 (1983).
- T. D. Read, S. N. Peterson, N. Tourasse, L. W. Baillie, I. T. Paulsen, K. E. Nelson, H. Tettelin, D. E. Fouts, J. A. Eisen, S. R. Gill, E. K. Holtzapple, O. A. Okstad, E. Helgason, J. Rilstone, M. Wu, J. F. Kolonay, M. J. Beanan, R. J. Dodson, L. M. Brinkac, M. Gwinn, R. T. DeBoy, R. Madpu, S. C. Daugherty, A. S. Durkin, D. H. Haft, W. C. Nelson, J. D. Peterson, M. Pop, H. K. Khouri, D. Radune, J. L. Benton, Y. Mahamoud, L. X. Jiang, I. R. Hance, J. F. Weidman, K. J. Berry, R. D. Plaut, A. M. Wolf, K. L. Watkins, W. C. Nierman, A. Hazen, R. Cline, C. Redmond, J. E. Thwaite, O. White, S. L. Salzberg, B. Thomason, A. M. Friedlander, T. M. Koehler, P. C. Hanna, A. B. Kolsto, and C. M. Fraser, "The genome sequence of *Bacillus anthracis* Ames and comparison to closely related bacteria," *Nature* **423**, 81–86 (2003).
- H. Barth, K. Aktories, M. R. Popoff, and B. G. Stiles, "Binary bacterial toxins: Biochemistry, biology, and applications of common clostridium and bacillus proteins," *Microbiol. Mol. Biol. Rev.* **68**, 373–402 (2004).
- J. Mogridge, K. Cunningham, D. B. Lacy, M. Mourez, and R. J. Collier, "The lethal and edema factors of anthrax toxin bind only to oligomeric forms of the protective antigen," *Proc. Natl. Acad. Sci. U.S.A.* **99**, 7045–7048 (2002).
- T. Candela, M. Mock, and A. Fouet, "CapE, a 47-amino-acid peptide, is necessary for *Bacillus anthracis* polyglutamate capsule synthesis," *J. Bacteriol.* **187**, 7765–7772 (2005).
- S. S. Rao, K. V. K. Mohan, and C. D. Atreya, "Detection technologies for *Bacillus anthracis*: Prospects and challenges," *J. Microbiol. Methods* **82**, 1–10 (2010).
- Z. A. Lai, Y. L. Wang, N. Allbritton, G. P. Li, and M. Bachman, "Label-free biosensor by protein grating coupler on planar optical waveguides," *Opt. Lett.* **33**, 1735–1737 (2008).
- X. D. Fan, I. M. White, S. I. Shopoua, H. Y. Zhu, J. D. Suter, and Y. Z. Sun, "Sensitive optical biosensors for unlabeled targets: A review," *Anal. Chim. Acta* **620**, 8–26 (2008).
- A. Ymeti, J. S. Kanger, J. Greve, P. V. Lambeck, R. Wijn, and R. G. Heideman, "Realization of a multichannel integrated Young interferometer chemical sensor," *Appl. Opt.* **42**, 5649–5660 (2003).
- B. H. Schneider, J. G. Edwards, and N. F. Hartman, "Hartman interferometer: versatile integrated optic sensor for label-free, real-time quantification of nucleic acids, proteins, and pathogens," *Clin. Chem.* **43**, 1757–1763 (1997).
- N. Skivesen, R. Horvath, S. Thinggaard, N. B. Larsen, and P. C. Pedersen, "Deep-probe metal-clad waveguide biosensors," *Biosens. Bioelectron.* **22**, 1282–1288 (2007).
- M. Zourab, S. Mohr, B. J. T. Brown, P. R. Fielden, M. B. McDonnell, and N. J. Goddard, "An integrated metal clad leaky waveguide sensor for detection of bacteria," *Anal. Chem.* **77**, 232–242 (2005).

15. A. N. Chryssis, S. S. Saini, S. M. Lee, H. M. Yi, W. E. Bentley, and M. Dagenais, "Detecting hybridization of DNA by highly sensitive evanescent field etched core fiber bragg grating sensors," *IEEE J. Sel. Top. Quantum Electron.* **11**, 864–872 (2005).
16. K. H. Smith, B. L. Ipson, T. L. Lowder, A. R. Hawkins, R. H. Selfridge, and S. M. Schultz, "Surface-relief fiber Bragg gratings for sensing applications," *Appl. Opt.* **45**, 1669–1675 (2006).
17. C. Y. Chao, W. Fung, and L. J. Guo, "Polymer microring resonators for biochemical sensing applications," *IEEE J. Sel. Top. Quantum Electron.* **12**, 134–142 (2006).
18. A. Ramachandran, S. Wang, J. Clarke, S. J. Ja, D. Goad, L. Wald, E. M. Flood, E. Knobbe, J. V. Hryniewicz, S. T. Chu, D. Gill, W. Chen, O. King, and B. E. Little, "A universal biosensing platform based on optical micro-ring resonators," *Biosens. Bioelectron.* **23**, 939–944 (2008).
19. B. T. Cunningham, P. Li, S. Schulz, B. Lin, C. Baird, J. Gerstenmaier, C. Genick, F. Wang, E. Fine, and L. Laing, "Label-free assays on the BIND system," *J. Biomol. Screen* **9**, 481–490 (2004).
20. E. Chow, A. Grot, L. W. Mirkarimi, M. Sigalas, and G. Girolami, "Ultra-compact biochemical sensor built with two-dimensional photonic crystal microcavity," *Opt. Lett.* **29**, 1093–1095 (2004).
21. D.-B. Wang, L.-J. Bi, Z.-P. Zhang, Y.-Y. Chen, R.-F. Yang, H.-P. Wei, Y.-F. Zhou, and X.-E. Zhang, "Label-free detection of *B. anthracis* spores using a surface plasmon resonance biosensor," *Analyst* **134**, 738–742 (2009).
22. J. Y. Ye, Y. Guo, T. B. Norris, and J. Baker, Jr. "Novel photonic crystal sensor," Patent No. 7,639,362 (2009).
23. Y. Guo, C. Divin, A. Myc, F. L. Terry, Jr., J. R. Baker, Jr., T. B. Norris, and J. Y. Ye, "Sensitive molecular binding assay using photonic crystal structure in total internal reflection," *Opt. Express* **16**, 11741–11749 (2008).
24. Y. Guo, J. Y. Ye, C. Divin, T. P. Thomas, A. Myc, T. F. Bersano-Begey, J. J. R. Baker, and T. B. Norris, "Real-time biomolecular binding detection using a sensitive photonic crystal biosensor," *Anal. Chem.* **82**, 5211–5218 (2010).
25. Y. L. Bai, C. G. Koh, M. Boreman, Y. J. Juang, I. C. Tang, L. J. Lee, and S. T. Yang, "Surface modification for enhancing antibody binding on polymer-based microfluidic device for enzyme-linked immunosorbent assay," *Langmuir* **22**, 9458–9467 (2006).
26. F. Fixe, M. Dufva, P. Telleman, C. B. V. Christensen, "Functionalization of poly(methyl methacrylate) (PMMA) as a substrate for DNA microarrays," *Nucleic Acids Res.* **32**, e9 (2004).
27. F. Kitagawa, K. Kubota, K. Sueyoshi, and K. Otsuka, "One-step immobilization of cationic polymer onto a poly(methyl methacrylate) microchip for high-performance electrophoretic analysis of proteins," *Sci. Technol. Adv. Mater.* **7**, 558–565 (2006).
28. M. Berndt, M. Lorenz, J. Enderlein, and S. Diez, "Axial nanometer distances measured by fluorescence lifetime imaging microscopy," *Nano Lett.* **10**, 1497–1500 (2010).
29. A. Driks, "Overview: development in bacteria: spore formation in *Bacillus subtilis*," *Cell. Mol. Life Sci.* **59**, 389–391 (2002).
30. J. Wang and M. Roehrl, "Anthrax vaccine design: strategies to achieve comprehensive protection against spore, bacillus, and toxin," *Med. Immunol.* **4**, 4 (2005).